Body-Shape Evolution among the Dragonfishes and Their Allies (Teleostei: Stomiiformes)

Authors: Gomes, Amanda Alves, Sidlauskas, Brian Lee, Machado, Fabio Andrade, Caires, Rodrigo Antunes, and Melo, Marcelo Roberto Souto de

Source: Ichthyology & Herpetology, 112(3) : 473-488

Published By: The American Society of Ichthyologists and Herpetologists

URL: https://doi.org/10.1643/i2023068

Ichthyology & Herpetology 112, No. 3, 2024, 473–488

Body-Shape Evolution among the Dragonfishes and Their Allies (Teleostei: Stomiiformes)

Amanda Alves Gomes[1], Brian Lee Sidlauskas[2], Fabio Andrade Machado[3], Rodrigo Antunes Caires[1], and Marcelo Roberto Souto de Melo[1]

The diverse deep-sea order Stomiiformes includes 457 species of mesopelagic and bathypelagic fishes with a remarkable diversity of structures associated with feeding, locomotion, and bioluminescence. This study investigates their patterns of body-shape evolution using geometric morphometry in an ecological and phylogenetic context. A total of 473 specimens from 56 different species in 48 genera representing all five families were photographed and 14 homologous landmarks and 50 semilandmarks were marked on the digital images. A principal component analysis (PCA) visualized body-shape variation, and morphological disparity analysis evaluated differences in variance among species in relation to their dietary classes, habitat partitioned by depth, and the presence or absence of diel vertical migration. The study also tested phylogenetic and ecological signals. The PCA revealed that variation in fin size and position, particularly for the dorsal and anal fins, accounted for the most important axis of variation among species. Changes in relative body size and body depth also contributed to morphological diversity. There is a trend toward body elongation in relation to depth distribution, with the meso-bathypelagic species having more elongated bodies than those restricted to the mesopelagic zone. Piscivorous and generalist species exhibit higher morphological disparity when compared to zooplanktivorous species, and meso- to bathypelagic species exhibit higher morphological disparity when compared to strictly mesopelagic species. A high phylogenetic signal indicates that morphological diversification within the Stomiiformes fits the expectations of Brownian evolution, in which the degree of shared ancestry rather than similarity of ecological niche predicts anatomical similarity. However, the current dataset may lack the statistical power to uncover any causal relationship between shifts in depth, diet, or migration and the shape diversification of stomiiforms.

THE order Stomiiformes comprises marine, bioluminescent fishes that inhabit the meso- and bathypelagic regions of the world's oceans, including the bristlemouths, lightfishes, marine hatchetfishes, dragonfishes, viperfishes, loosejaws, and snaggletooths (Harold, 2002; Nelson et al., 2016). There are currently 457 valid species allocated to the families Diplophidae (10 species), Gonostomatidae (24 species), Phosichthyidae (24 species), Sternoptychidae (78 species), and Stomiidae (321 species; Nelson et al., 2016; Fricke et al., 2023). Stomiiforms represent one of the most diversified radiations of deep-sea fishes, having a remarkable array of body shapes, sizes, and structures associated with feeding, locomotion, and bioluminescence, including head length, size and position of the mouth, dentition, eye size, position of fins, presence or absence of a barbel associated with the hyoid arch, and presence or absence of an adipose fin (Harold and Weitzman, 1996; Harold, 2002; Kenaley, 2009; Fig. 1). Their luminescent organs include body photophores arranged in rows or distributed irregularly, and sometimes large orbital photophores and/or a bioluminescent lure at the tip of the barbel (Herring, 2007; Kenaley et al., 2014; Marranzino and Webb, 2018). Stomiiforms also represent key members of the oceanic food web, as they are abundant, and most species perform diel vertical migrations to feed in shallow waters during the night, transporting energy and carbon to the deeper layers during daytime (Young et al., 1997; Gannon et al., 1998; Sutton, 2013; Carmo et al., 2015; Eduardo et al., 2020).

Although the remarkable adaptations of deep-sea fishes to the environment have captivated the attention of scientists and the public for centuries, only a few studies on their ecomorphology and body-shape evolution have adopted a quantitative approach (e.g., Orlov and Binohlan, 2009; Neat and Campbell, 2013; Denton and Adams, 2015; Farré et al., 2016; Mindel et al., 2016; Tuset et al., 2018; Maile et al., 2020; Martinez et al., 2021). Recent studies suggested that variation in depth preference strongly influences the diversification of lizardfishes (Maile et al., 2020) and deep-sea fishes generally (Martinez et al., 2021), increasing the morphological disparity with the depth. Variation in factors such as turbulence, habitat complexity, and sunlight levels in the deeper layers of the ocean create opportunities for the evolution of unique morphological adaptations in the deep ocean (Martinez et al., 2021).

Indeed, because of their morphological adaptations, species richness, depth distribution, feeding habits, and migratory behavior, the stomiiforms represent an interesting case study to further understand the evolution of deep-sea organisms in relation to environmental changes (Angel, 1997; Thistle, 2003; Mindel et al., 2016). In a comprehensive study about the ecomorphology of deep-sea fishes, Martinez et al. (2021) included many stomiiform species (~70

[1] Laboratório de Diversidade, Ecologia e Evolução de Peixes–DEEP Lab, Instituto Oceanográfico, Universidade de São Paulo, São Paulo, São Paulo 05508-120, Brazil; Email: (AAG) amanda_gomes@alumni.usp.br; (RAC) rodricaires@yahoo.com.br; and (MRSM) melomar@usp.br. Send correspondence to AAG.

[2] Department of Fisheries, Wildlife and Conservation Sciences, Oregon State University, Corvallis, Oregon 97331; Email: brian.sidlauskas@oregonstate.edu.

[3] Department of Integrative Biology, Oklahoma State University, Stillwater, Oklahoma 74078; Email: fabio.machado@okstate.edu.

Submitted: 25 August 2023. Accepted: 19 June 2024. Associate Editor: M. T. Craig.

 DOI: 10.1643/i2023068 Published online: 30 October 2024

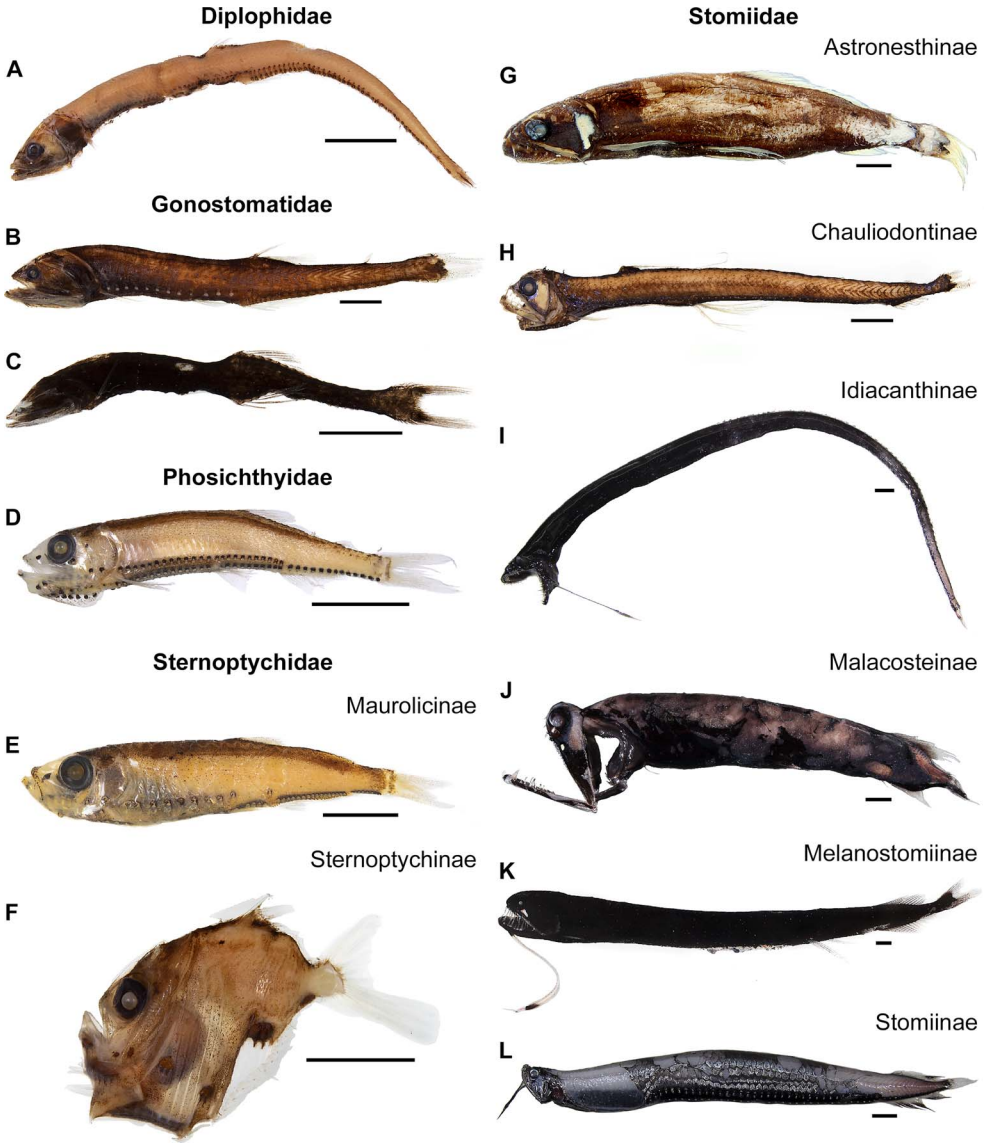

Fig. 1. Body-shape diversity among the Stomiiformes, with representatives of all five families. (A) *Diplophos taenia*, MZUSP 80530, 74.4 mm SL; (B) *Sigmops elongatus*, MZUSP 129718, 102.4 mm SL; (C) *Cyclothone pseudopallida*, MZUSP 129716, 49.7 mm SL; (D) *Vinciguerria nimbaria*, MZUSP 129723, 44.7 mm SL; (E) *Maurolicus stehmanni*, MZUSP 80266, 47.1 mm SL; (F) *Sternoptyx pseudodiaphana*, MZUSP 129730, 32.0 mm SL; (G) *Astronesthes macropogon*, MZUSP 80272, 115.6 mm SL; (H) *Chauliodus danae*, MZUSP 128733, 95.6 mm SL; (I) *Idiacanthus atlanticus*, MZUSP 129883, 295.0 mm SL; (J) *Malacosteus australis*, MZUSP 129908, 129.0 mm SL; (K) *Melanostomias melanops*, MZUSP 129903, 193.6 mm SL; (L) *Stomias affinis*, MZUSP 129880, 173.0 mm SL. Scale bars = 10 mm.

species) but did not focus on the order and examined only eight linear traits and a single environmental variable (depth). No modern ecomorphological study has applied geometric morphometrics to comprehensively capture and statistically quantify the intricate forms within the entire order, which would aid the examination of evolutionary hypotheses within a phylogenetic and ecological context (Goswami et al., 2019).

In this study, we apply geometric morphometric analyses to reconstruct patterns of body-shape evolution among the stomiiforms. Specifically, the study aims to (1) elucidate the main correlates of stomiiform morphological disparity; (2) determine whether major axes of stomiiform body-shape diversity are associated with dietary preferences, bathymetric distribution, and diel vertical migration patterns; and (3) quantify the phylogenetic signal in stomiiform body shape.

MATERIALS AND METHODS

Taxonomic sampling.—Specimens were obtained from the scientific collections of Museu de Zoologia, Universidade de São Paulo (MZUSP), Museu Nacional, Universidade Federal do Rio de Janeiro (MNRJ), Oregon State University Ichthyology Collection (OS), Museum of Comparative Zoology, Harvard University (MCZ), Scripps Institution of Oceanography, University of California San Diego (SIO), and the National Museum of Natural History, Smithsonian Institution (USNM). Some additional specimens were collected during oceanographic cruises in the Southwest Atlantic conducted onboard the RV *Alucia* in 2017 and by the RV *Alpha Crucis* in 2019 and 2022, the latter as part of the DEEP-OCEAN Project. In total, 473 specimens from 56 species were used, representing 48 out of the 53 stomiiform genera and all five families (Table 1).

Only adult specimens in good condition were chosen, and at least five specimens per species were selected, except in 18 (33%) cases where fewer than five specimens in good condition were available (Table 1). For each specimen, the left side was photographed using a digital SLR camera (Nikon D500 with a 60 mm lens or Nikon D3200 with an 18–55 mm lens). For each specimen, the standard length (SL) was measured using a digital caliper to the nearest 0.1 mm.

Ecological data.—For each species, information about diet, bathymetric distribution, and the presence or absence of

Table 1. List of the species of Stomiiformes examined, including the number of specimens (*n*), minimum and maximum standard length, and depth of capture.

Species	*n*	Size (mm SL)	Depth (m)
Diplophidae (2)			
Diplophos taenia Günther, 1873	8	69.8–145.7	132–1,300
Manducus maderensis (Johnson, 1890)	21	77.4–191.9	55–927
Gonostomatidae (6)			
Cyclothone microdon (Günther, 1878)	9	32.9–50.8	830–2,850
Cyclothone pseudopallida Mukhacheva, 1964	14	31.0–55.7	1,000
Gonostoma atlanticum Norman, 1930	2	58.6–59.0	3,050
Margrethia obtusirostra Jespersen and Tåning, 1919	5	41.3–80.0	425–575
Sigmops elongatus (Günther, 1878)	24	51.2–159.9	517–1,648
Zaphotias pedaliotus (Goode and Bean, 1896)	8	38.4–69.1	500–2,300
Phosichthyidae (7)			
Ichthyococcus elongatus Imai, 1941	4	27.5–93.1	200–2,450
Phosichthys argenteus Hutton, 1872	15	64.5–237.2	517–1,141
Pollichthys mauli (Poll, 1953)	15	40.6–49.7	445–917
Polymetme thaeocoryla Parin and Borodulina, 1990	25	33.8–162.6	438–605
Vinciguerria nimbaria (Jordan and Williams, 1895)	23	31.6–44.5	200–1,270
Vinciguerria poweriae (Cocco, 1838)	8	30.4–36.2	1,480
Yarrella blackfordi Goode and Bean, 1896	3	150.7–188.5	388–880
Sternoptychidae (12)			
Araiophos eastropas Ahlstrom and Moser, 1969	4	275.0–297.0	No info.
Argyripnus atlanticus Maul, 1952	10	49.8–71.6	415
Argyropelecus aculeatus Valenciennes, 1850	14	32.6–70.3	445–1,000
Argyropelecus affinis Garman, 1899	8	41.3–72.7	406–2,400
Danaphos oculatus (Garman, 1899)	3	33.5–42.1	310–2,400
Maurolicus stehmanni Parin and Kobyliansky, 1993	10	32.5–41.8	610
Maurolicus weitzmani Parin and Kobyliansky, 1993	2	43.5–58.3	219–347
Polyipnus laternatus Garman, 1899	2	40.8–43.1	457–611
Polyipnus spinifer Borodulina, 1979	3	46.4–59.1	465
Sternoptyx pseudobscura Baird, 1971	22	28.4–51.3	904–2,450
Thorophos nexilis (Myers, 1932)	1	59.4	320
Valenciennellus tripunctulatus (Esmark, 1871)	2	22.4–25.1	830–1,000
Stomiidae (29)			
Aristostomias scintillans (Gilbert, 1915)	7	102.4–122.3	50–4,300
Astronesthes gemmifer Goode and Bean, 1896	2	130.2–151.7	1,266
Astronesthes macropogon Goodyear and Gibbs, 1970	17	70.9–130.0	635–1,799
Bathophilus flemingi Aron and McCrery, 1958	12	56.4–67.1	160–2,520
Borostomias antarcticus (Lönnberg, 1905)	7	77.1–286.5	1,230–2,000
Chauliodus danae Regan and Trewavas, 1929	2	103.6–108.5	1,000
Chauliodus macouni Bean, 1890	13	67.0–190.1	200–1,000
Chauliodus sloani Bloch and Schneider, 1801	4	95.6–166.6	599–1,089
Chirostomias pliopterus Regan and Trewavas, 1930	2	120.3–157.7	1,000–1,016
Echiostoma barbatum Lowe, 1843	5	99.3–257.7	760–1,332
Eustomias filifer (Gilchrist, 1906)	3	73.4–107.4	90–200
Flagellostomias boureei (Zugmayer, 1913)	6	72.4–184.0	50–1,000
Grammatostomias flagellibarba Holt and Byrne, 1910	2	32.2–202.7	800–1,636
Heterophotus ophistoma Regan and Trewavas, 1929	8	57.7–236.9	200–1,850
Idiacanthus atlanticus Brauer, 1906	8	188.0–353.0	517–1,141
Leptostomias gladiator (Zugmayer, 1911)	6	101.0–183.6	170–1,354
Malacosteus australis Kenaley, 2007	10	130.8–195.7	616–1,637
Melanostomias melanops Brauer, 1902	9	153.0–206.6	666–1,545
Neonesthes capensis (Gilchrist and von Bonde, 1924)	2	153.4–153.6	592
Odontostomias micropogon Norman, 1930	4	195.2–221.3	400–740
Opostomias mitsuii Imai, 1941	11	116.3–128.1	50–1,500
Pachystomias microdon (Günther, 1878)	5	123.9–190.2	1,900–2,200
Photonectes margarita (Goode and Bean, 1896)	7	73.4–199.6	80–2,400
Photostomias guernei Collett, 1889	6	80.1–107.4	125
Rhadinesthes decimus (Zugmayer, 1911)	3	133.9–225.8	1,300–2,633

Table 1. Continued.

Species	*n*	Size (mm SL)	Depth (m)
Stomias affinis Günther, 1887	17	79.9–190.9	506–1,200
Tactostoma macropus Bolin, 1939	23	114.8–132.2	200–1,380
Thysanactis dentex Regan and Trewavas, 1930	5	111.6–162.2	1,500–4,000
Trigonolampa miriceps Regan and Trewavas, 1930	3	172.9–233.2	915–1,830

diel vertical migration (DVM) were obtained from the literature or from the precise collection data contained on the label and coded as discrete categories according to the categories given below (Supplemental Table 1; see Data Accessibility). Species diet was sorted into three classes: Type 1 includes zooplanktivores that feed primarily on small crustaceans, such as copepods, euphausiids, ostracods, mysids, cladocerans, and amphipods; Type 2 includes generalists that feed on both crustaceans and fishes; and Type 3 includes exclusively piscivores. The species were divided into two categories according to their bathymetric distributions: mesopelagic species occur between 200 and 1,000 meters of depth; and meso-bathypelagic species can be found in both the mesopelagic zone and deeper than 1,000 meters depth. The species were also classified as migratory or non-migratory based on the presence or absence of DVM, respectively. The environmental data were converted into factors and used as classifiers in downstream analyses. Classification follows Nelson (2006) except for the recognition of a distinct Chauliodontinae following Fricke et al. (2023).

Geometric morphometrics.—A landmark-based geometric morphometric approach was used to quantify variation in body shape using the tps series of programs (Rohlf, 2015, 2018). We located 14 fixed landmarks on homologous structures (Table 2) and interpolated 50 semilandmarks in tpsDig2 (Rohlf, 2018), thereby adapting the method of several other studies (Nunes et al., 2008; Pulcini et al., 2008; Farré et al., 2015; Maile et al., 2020) to stomiiform morphology (Fig. 2). We did not include a landmark on the lower jaw because of variation in the position of fixation. We excluded the ventrum because of marked shape changes due to variation in stomach fullness.

Table 2. Descriptions of the 14 homologous landmarks.

Landmark	Description
1	Tip of the snout at anterior tip of premaxilla
2	Distal tip of maxilla
3	Upper eye margin
4	Lower eye margin
5	Ventralmost point of opercle
6	Dorsalmost point of preopercle
7	Dorsal margin of skull vertically aligned to the orbit
8	Dorsal-fin origin at base of the anteriormost ray
9	Dorsal-fin insertion at base of posteriormost ray
10	Pelvic-fin origin at base of the anteriormost ray
11	Anal-fin origin at base of the anteriormost ray
12	Anal-fin insertion at base of the anteriormost ray
13	Caudal peduncle at base of the anteriormost dorsal procurrent ray
14	Caudal peduncle at base of the anteriormost ventral procurrent ray

The landmark coordinates were submitted to a generalized Procrustes analysis (GPA) using the geomorph package version 4.0.5 (Baken et al., 2021) in R (R Core Team, 2023). This analysis scales the Cartesian coordinates to a common centroid size and rotates the configurations to minimize the sum of the square distances between the corresponding landmarks, thereby removing the information on isometric size, position, and spatial orientation (Bookstein, 1991).

Principal component analysis, Procrustes ANOVA, and morphological disparity.—A principal component analysis (PCA) using specimens was conducted in the geomorph package version 4.0.5 (Baken et al., 2021) and plotted with ggplot2 package version 3.4.3 (Wickham, 2016) according to each classifier: clades, diet, depth range, and DVM. Extremes of the negative and positive shape variation on each of the first several principal component axes were plotted using the function 'plotRefToTarget' from the geomorph package.

Morphometric data were averaged by group (classifiers) using the function 'two.d.array' from the geomorph package. This function converts a ($p \times k \times n$) array of landmark coordinates into a two-dimensional matrix ($n \times [p \times k]$), resulting in an array of species means. We then performed the generalized Procrustes analysis with the species means. A Procrustes ANOVA was performed using the 'procD.lm' function (geomorph), with 500 permutations, to assess whether a set of species with different clades, diets, depth ranges, and migratory behaviors differed significantly in shape. This analysis also tested for an allometric effect between body shape and species size. The morphological disparity based on Procrustes variance among stomiiforms in each clade, diet class, migration class, and depth class were calculated using the function 'morphol.disparity' (geomorph) based on 1,000 randomized residual permutations. We repeated all analyses with outliers excluded (defined as species with high Procrustes distance from the mean shape).

Phylomorphospace, phylogenetic signal, and phylogenetic ANOVA.—A phylogenetic hypothesis for 99 stomiiform species was extracted from the time-calibrated phylogenetic tree of ray-finned fishes produced by Rabosky et al. (2018) and distributed via the Fish Tree of Life website (https://fishtreeoflife.org/). The phylogeny was linked to the PCA results in phytools version 1.5-1 (Revell, 2012) to create a

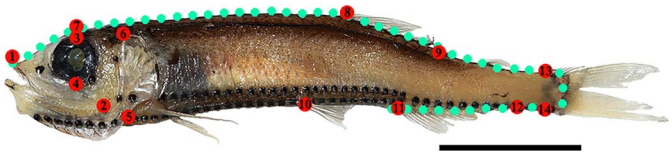

Fig. 2. The position of the 14 fixed landmarks (red) and 50 semilandmarks (green) illustrated on *Vinciguerria nimbaria*, MZUSP 129723, 38.6 mm SL. Scale bar = 10 mm.

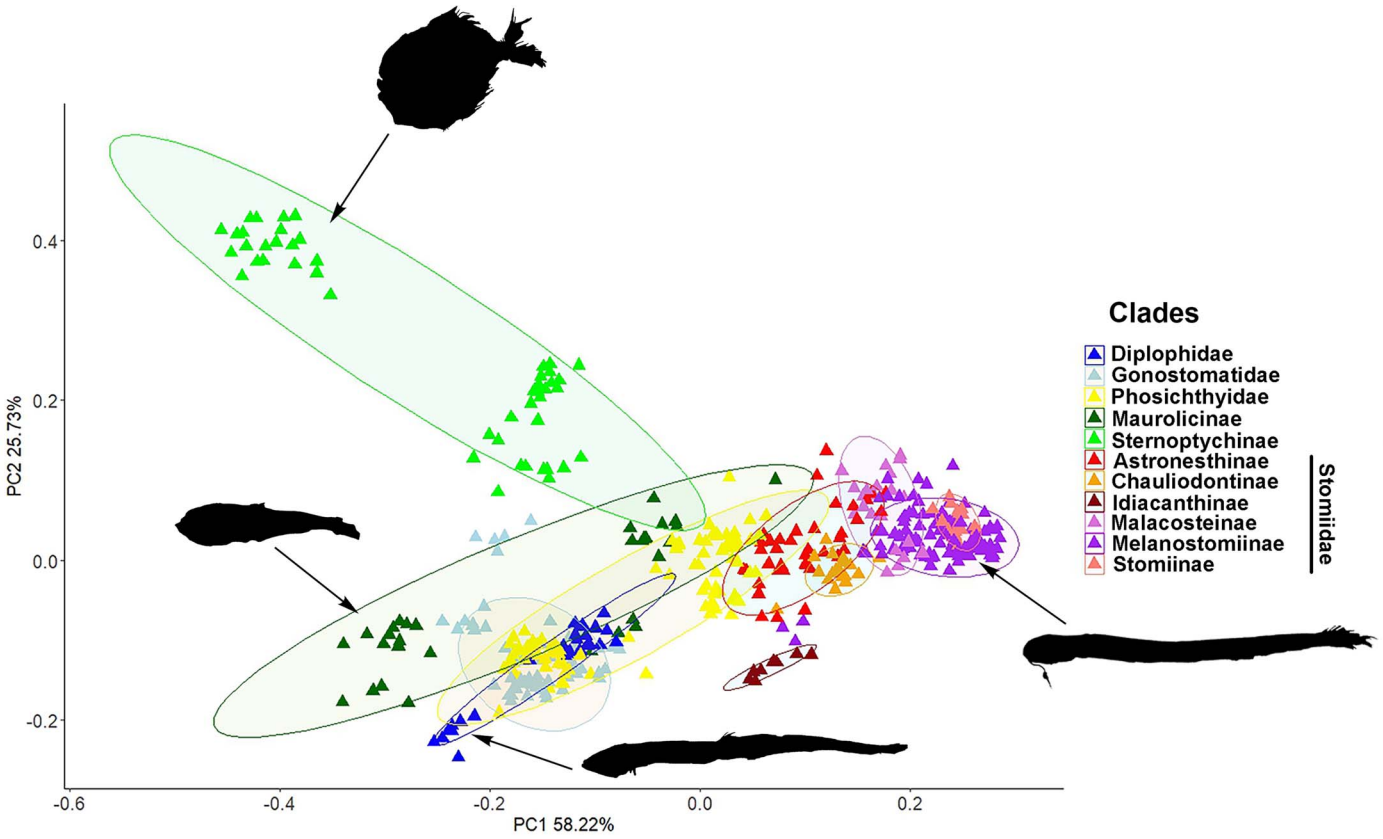

Fig. 3. The first and second axes of a principal component analysis (PCA) in the Stomiiformes, based on 473 specimens. Colored ellipses represent distribution of specimens within stomiiform taxonomic groups.

genus-level phylomorphospace (Sidlauskas, 2008). In cases when we did not have access to the exact same species used by Raboksy et al. (2018), we substituted a closely related congener for which we had morphological data. Taxa for which we had no morphological data were trimmed using the 'drop.tip' function from the ape package version 5.7-1 (Paradis et al., 2004), and we further pruned the tree to include a single species in each genus. Supplemental Table 2 (see Data Accessibility) details the species selected for the phylomorphospace.

The phylogenetic signal of body shape and centroid size was assessed using the 'physignal' function from geomorph (Baken et al., 2021). That approach uses a multivariate generalization of Blomberg's *K* which measures phylogenetic signal by calculating a ratio of the observed trait variance relative to the value estimated at the root of the tree and the trait variance expected under Brownian motion (Blomberg et al., 2003). The resulting *K*mult statistic was compared to a null distribution generated from 1,000 random permutation tests using the average shapes of species. We used phylogenetic ANOVA on the species-averaged Procrustes coordinates to test for an allometric effect between body shape and species size and for significant differences among the diet, depth, and migration classes. This analysis used the 'procD.pgls' function in geomorph with 500 permutations.

RESULTS

Principal component analysis.—The PCA revealed significant multivariate variation in stomiiform body shape. We examined the eigenvalues to determine the number of principal components to be considered. The first three PCA axes collectively account for 92.42% of the total variance among individual specimens, mostly on the first two principal components (Fig. 3). The observed shape variation includes notable shifts in the dorsal- and anal-fin position, dorsal- and anal-fin size, and the head and body proportions.

Axis 1, which explains 58.22% of the variance, describes the positions of the dorsal, anal, and pelvic fins, the lengths of the anal fin and head, the caudal-peduncle depth, and eye diameter. Species exhibiting midline placement of the dorsal fin, a long anal fin, pelvic fin positioned closer to the midline of the body, and a larger eye have negative PC1 values. In contrast, species with a posterior placement of the dorsal and anal fins, a sagittiform body shape, pelvic fin placed posteriorly on body, and moderate-sized eye exhibit positive PC1 values. The species with the most extreme negative PC1 values include the sternoptychids *Argyripnus atlanticus*, *Danaphos oculatus*, *Sternoptyx pseudobscura*, *Thorophos nexilis*, and *Valenciennellus tripunctulatus*, while those with extreme positive PC1 values include the melanostomiines *Melanostomias melanops*, *Tactostoma macropus*, *Thysanactis dentex*, and the stomiine *Stomias affinis* (Fig. 4).

Axis 2, which explains 25.73% of the variance, showcases variation in body depth, body length, the size and shape of the head, anal-fin size, and pelvic-fin position. Negative PC2 values reflect species with deeper bodies, pelvic fins positioned posteriorly on body, shorter anal fins, and larger eyes. In contrast, positive PC2 values reflect species with longer, slender bodies that are flattened dorsoventrally,

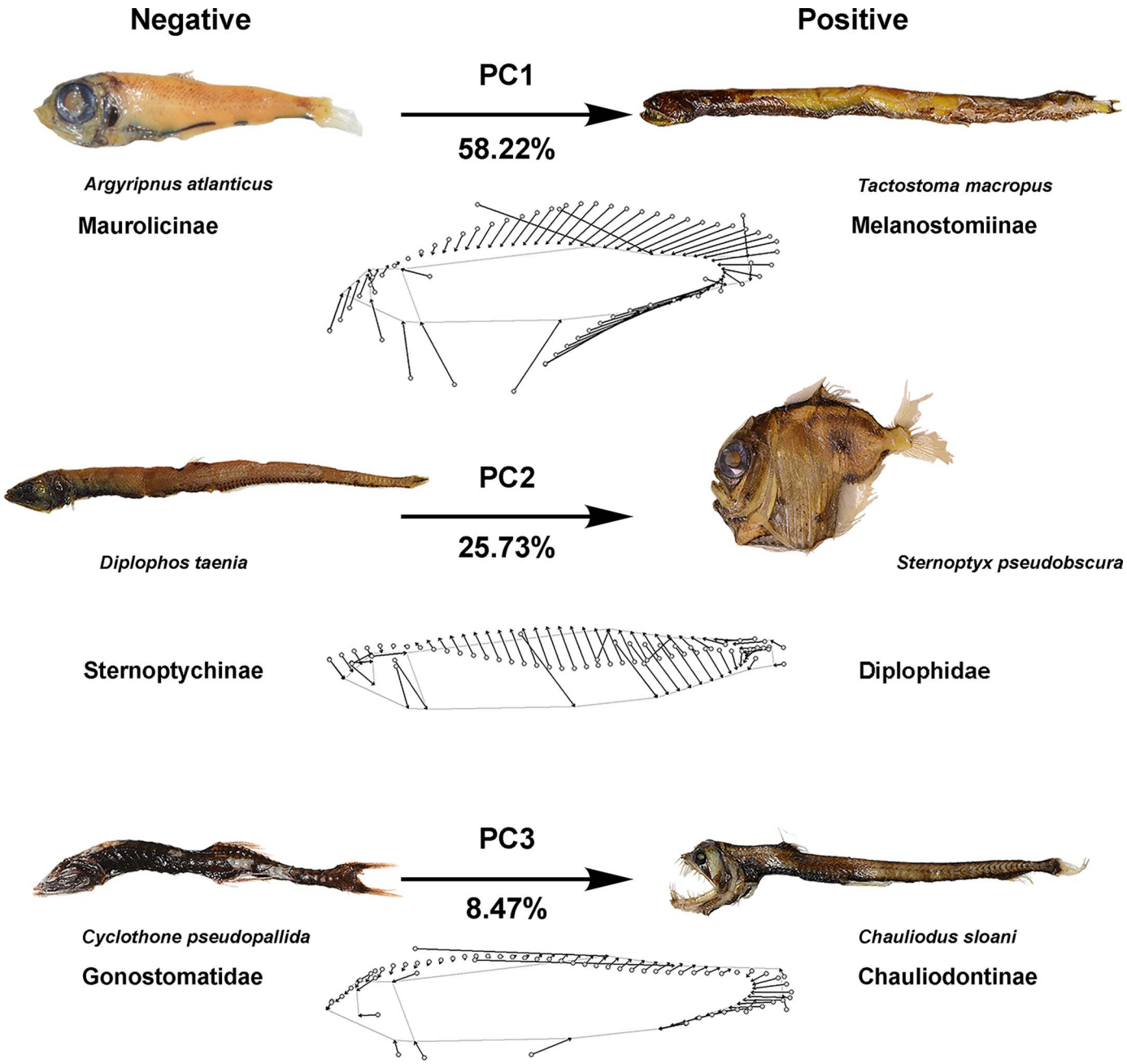

Fig. 4. Stomiiform species at the negative and positive extremes of body-shape variation along the first three principal component axes. Wireframes represent the average body shape, and vectors represent the average configuration warped to an extreme observed value of the corresponding PC axis. The percentage of total variance represented by each axis is indicated between the two extreme shapes.

pelvic fins positioned at the midline of the body, longer anal fins, and smaller eyes (Fig. 3). Notably, sternoptychines such as *Argyropelecus aculeatus* and *Sternoptyx pseudobscura* have extreme negative PC2 values, while the diplophid *Diplophos taenia* occupies the positive extreme of PC2 (Fig. 4).

Axis 3, which explains 8.47% of the shape variance, is strongly influenced by the position of the dorsal and pelvic fins. Negative PC3 values indicate species with the dorsal fin positioned posteriorly on the body and the pelvic fin positioned near the anal fin. In contrast, species with the dorsal fin closer to midbody and the pelvic fin more anterior have positive PC3 values. The melanostomiine *Eustomias filifer* and the gonostomatids *Cyclothone microdon* and *C. pseudopallida* occupy the negative extreme of PC3 values, while the chauliodontines *Chauliodus macouni* and *C. sloani* occupy the positive extreme (Fig. 4).

Stomiiform species with different diets and bathymetric distributions tend to occupy distinct regions of morphospace (Fig. 5). The piscivorous stomiids (type 3 diet) occupy the positive extreme of PC1 (Fig. 5A) and have sagittiform bodies, large mouths, and premaxillae armed with widely spaced fangs. Zooplanktivorous species (type 1 diet) mostly occupy the lower left corner of morphospace with negative values for PC1 and PC2, including diplophids, gonostomatids, maurolicines, and most phosichthyids, which have fusiform or elongated bodies, moderate to large mouths

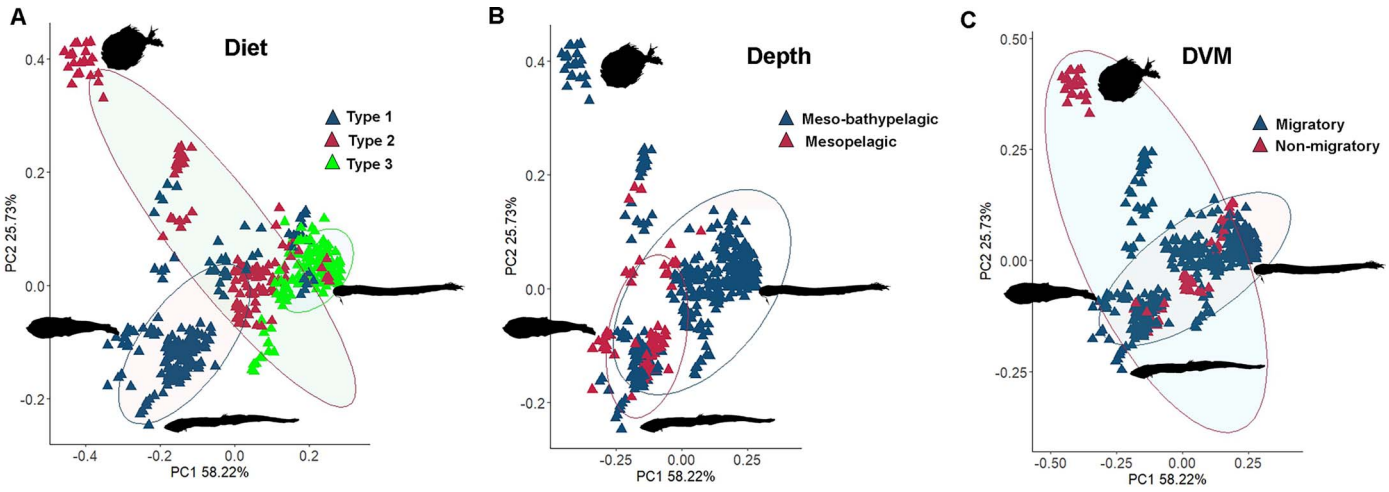

Fig. 5. The first and second morphospace axes, color coded by (A) diet, (B) bathymetric distribution, and (C) diel vertical migration pattern (DVM).

armed with numerous minute teeth, and eye sizes varying from small to large. Generalist species that feed upon crustaceans and fishes (type 2 diet) occur across the entire range of PC1 and have a variable morphology with a deep or fusiform body, and a moderate to large mouth armed with numerous teeth of variable sizes. These include most astronesthines and the phosichthyids *Phosichthys argenteus* and *Vinciguerria nimbaria*. Sternoptychines are also generalists but occupy the upper left quadrant of morphospace, where the positive PC2 values reflect their deep bodies.

Regarding the bathymetric distribution (Fig. 5B), most mesopelagic fishes have fusiform bodies with negative PC1 values, such as the maurolicines. In contrast, meso- to bathypelagic species such as gonostomatids, stomiids, and most phosichthyids are more diverse and occupy the entire range of observed morphology. In regard to DVM, no clear association with body shape emerged as most species migrate on a daily basis. (Fig. 5C).

Morphological disparity and Procrustes ANOVA.—The morphological disparity of the astronesthines, chauliodontines, phosichthyids, and sternoptychines differs significantly ($P \leq 0.05$) from all other families and subfamilies, with sternoptychines (hatchetfishes) and some chauliodontines (viperfishes) being significantly more diverse (Procrustes variance 0.19 and 0.09, respectively), and astronesthines (snaggletooths) and phosichthyids (lightfishes) significantly less diverse (Procrustes variance 0.02 for both groups).

Groups of stomiiform species with different ecologies (diet, depth, and DVM) differ in morphological disparity. Specifically, the body-shape disparity of meso-bathypelagic stomiiforms exceeds that of mesopelagic stomiiforms, non-migratory species are more disparate than migratory ones, and generalists are more disparate than are zooplanktivores or piscivores (Table 3).

The body shape of stomiiforms differs significantly among subclades and diet classes (Procrustes ANOVA, $P \leq 0.05$). In contrast, no significant relationship was found between shape and ocean depth or DVM. Similarly, no significant relationships between centroid size (CS) and any classifier were uncovered (Table 4).

Phylogenetic signal, phylomorphospace, and phylogenetic ANOVA.—Significant phylogenetic signal exists for stomiiform body shape ($K = 1.9275$, $P = 0.001$) and centroid size ($K = 1.0341$, $P = 0.03$; Supplemental Fig. 1A, B; see Data Accessibility). Those values indicate that body size variation closely approximates the Brownian expectation, while for body shape, closely related lineages tend to resemble each other even more than one would expect from a random walk.

When visualized in a phylomorphospace, closely related taxa clearly tend to cluster closely and distant related taxa diverge, which corroborates the numerical estimate of strong phylogenetic signal in body shape. Most stomiids occupy the same region of phylomorphospace as the other members of their families, except for the chauliodontine *Chauliodus*, the idiacanthine *Idiacanthus*, and the astronesthines, especially *Astronesthes*, *Neonesthes*, and *Rhadinesthes*. Those five taxa diverge from the other members of their families in body shapes and dorsal-fin position. The Chauliodontinae have an anteriorly placed dorsal fin unlike the posterior dorsal fin that characterizes most stomiids or the midbody placement typical of astronesthines. Idiacanthines have anguilliform bodies with long dorsal and anal fins vs. elongated or fusiform bodies with short dorsal and anal fins in most of the other stomiids. Astronesthines have fusiform bodies with the dorsal fin at midbody, while most stomiids have elongated bodies with posteriorly placed dorsal fins except in idiacanthines, as described above.

The main overlap in phylomorphospace was found between astronesthines and the phosichthyids *Ichthyococcus*, *Phosichthys*, and *Vinciguerria*. The remaining phosichthyids *Pollichthys*, *Polymetme*, and *Yarrella* share a region of phylomorphospace with

Table 3. Stomiiformes Procrustes variance and *P*-values of the morphological disparity test by diet, depth, and diel vertical migration (DVM). Asterisks indicate statistically significant differences at $P \leq 0.05$.

Classifiers	Procrustes variance	*P*-values
Diet: Type 1	0.048	0.001*/0.042*
Diet: Type 2	0.084	0.001*/0.013*
Diet: Type 3	0.063	0.042*/0.013*
Depth: Mesopelagic	0.044	0.009*
Depth: Meso-bathypelagic	0.066	0.009*
DVM: Migratory	0.051	0.001*
DVM: Non-migratory	0.114	0.001*

Table 4. Results from Procrustes ANOVA testing for differences in mean body shape and centroid size (CS) among stomiiforms classified by clades, diel vertical migration (DVM), bathymetric distribution (depth), and diet. Asterisks represent significant differences ($P \leq 0.05$).

	F-values		*P*-values	
Classifiers	Shape	CS	Shape	CS
Clades	7.90	4.24	0.002*	0.092
DVM	0.79	0.16	0.454	0.762
Depth	1.97	0.29	0.122	0.262
Diet	14.4	1.01	0.002*	0.23

the gonostomatids. Sternoptychids have a broad distribution in the phylomorphospace, with some sternoptychines such as *Sternoptyx* occupying a distinct region in the lower right corner of morphospace distant from all other stomiiforms (Fig. 6).

Phylogenetically adjusted tests for differences in morphological disparity among ecological classes and clades returned universally insignificant results ($P > 0.05$; Table 5). Likewise, the phylogenetic Procrustes ANOVA uncovered no significant differences in size or shape between stomiiforms grouped by ecological traits or by subclade ($P > 0.05$; Table 6). However, these tests used substantially smaller sample sizes than did the non-phylogenetic tests reported above (Fig. 7), and the lack of significance must not be taken as proof of a lack of relationship.

DISCUSSION

Stomiiform body-shape patterns.—Stomiiforms vary substantially in body shape, with the three main PCA axes describing important variation in body shape associated with feeding habits and depth range. Fin dimensions and positions, particularly the dorsal and anal fins, hold sway over the primary variances in the body shapes among stomiiforms, followed by the relative body length and height. The two main PCA axes summarize differences between species with the dorsal fin positioned at midbody, anterior to the anal-fin origin, anal fin long, and deep-bodied or fusiform body shapes (e.g., maurolicines and sternoptychines) to species with a dorsal fin posterior on body, parallel to a shorter anal fin, with elongated body (e.g., melanostomiines and stomiines; Fig. 3). Six main clusters of stomiiform body shapes emerged: (1) Body fusiform with a long anal fin is present in the maurolicines *Argyripnus*, *Danaphos*, *Thorophos*, and *Valenciennellus*, and in the gonostomatids *Margrethia* and *Zaphotias* at negative PC1 and PC2. (2) Body fusiform with a short anal fin is present in astronesthines (except in *Rhadinesthes*), in the phosichthyids *Ichthyococcus*, *Phosichthys*, and *Vinciguerria*, and in the maurolicine *Maurolicus* at consensus configuration. (3) Body deep and laterally compressed is present in sternoptychines at negative PC1 and positive PC2. All stomiiform clades have evolved some elongated members, particularly the Stomiidae. (4) Body elongated with a moderate to long anal fin is present in diplophids, in the gonostomatids *Cyclothone*, *Gonostoma*, and *Sigmops*, in the phosichthyids *Pollichthys*, *Polymetme*, and *Yarrella*, in the astronesthine *Rhadinesthes*, and in the maurolicine *Araiophos* at negative PC1 and PC2. (5) Body elongated and sagittiform, with the anal fin short, posterior on the body and parallel to the dorsal fin is present in stomiines, malacosteines, and most melanostomiines at positive PC1. (6) Body anguilliform with an extremely elongated dorsal and long anal fin is present only in *Idiacanthus atlanticus* at positive PC1 and negative PC2. *Idiacanthus atlanticus* clustered next to the melanostomiine *Eustomias filifer* in the morphospace. Though the latter does not possess an anguilliform body shape, it does have a long anal fin

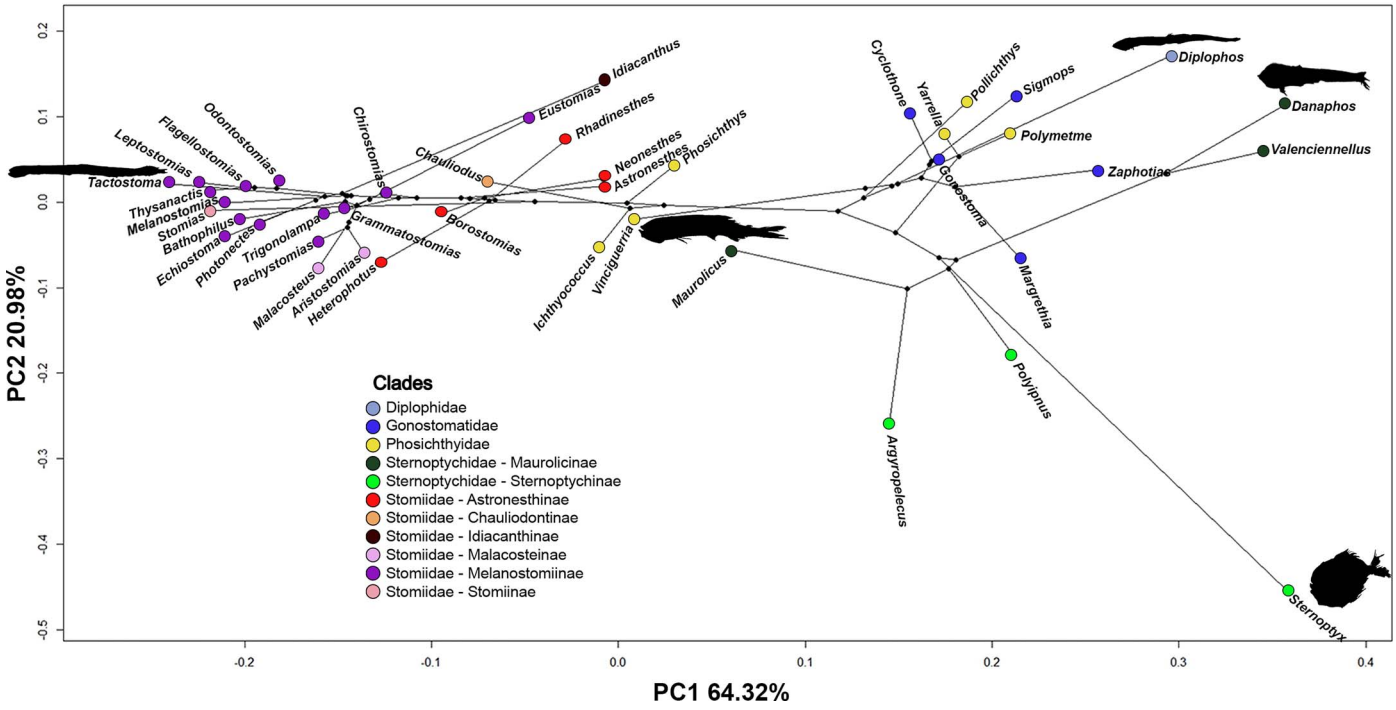

Fig. 6. Genus-level phylomorphospace based on the time-calibrated phylogeny of Rabosky et al. (2018), color coded by stomiiform taxonomic groups.

Table 5. Procrustes variance and *P*-values of the morphological disparity in Stomiiformes without and with accounting for phylogeny. Asterisks represent significant morphological disparity ($P \leq 0.05$).

	Without phylogeny		With phylogeny	
Classifiers	Procrustes variance	*P*-values	Procrustes variance	*P*-values
Diet: Type 1	0.048	0.001*/0.042*	0.056	0.389/0.597
Diet: Type 2	0.084	0.001*/0.013*	0.039	0.389/0.677
Diet: Type 3	0.063	0.042*/0.013*	0.047	0.597/0.677
Depth: Mesopelagic	0.044	0.009*	0.054	0.756
Depth: Meso-bathypelagic	0.066	0.009*	0.048	0.756
DVM: Migratory	0.051	0.001*	0.050	0.667
DVM: Non-migratory	0.114	0.001*	0.041	0.667

that contrasts with the short anal fin present on the other melanostomiines (Fig. 3).

Chauliodus and the Astronesthinae clustered in the same region of morphospace, at positive PC1 (Fig. 3). These species share dorsal fin anteriorly positioned, contrasting with the other stomiids, which have the dorsal fin posteriorly placed. *Chauliodus* is unique in many aspects: its body shape is elongated with a long anal fin, similar to that in stomiines, malacosteines, and melanostomiines; however, the dorsal fin is anteriorly positioned, with an elongated dorsal-fin ray and a bioluminescent lure at its tip—similar to the modified esca and lure present on the dorsal fin of anglerfishes (Lophiiformes; Tchernavin, 1953; Clarke, 1982; Gartner et al., 1997; Pietsch, 2009). Nevertheless, chauliodontines have a large adipose fin, posteriorly placed, parallel to the anal fin resulting in a sagittiform body shape like most stomiids since, presumably, the combined fin area well posterior on the body generates a large amount of burst-speed thrust for prey capture (Webb, 1984; Fink, 1985). In contrast, most astronesthines have the dorsal fin positioned near the midbody (Weitzman, 1967; Parin and Borodulina, 2003). However, in *Heterophotus*, the dorsal-fin origin is somewhat posteriorly placed, but not parallel to the anal fin (Weitzman, 1967; Fink, 1985), while in *Astronesthes* the dorsal-fin position varies from midbody to posteriorly placed among the species (Parin and Borodulina, 2003).

Our results provide evidence that elongation is the second major axis of stomiiform body-shape diversification, and these results are consistent with previous investigations conducted on ecologically diverse clades of teleosts, such as marine benthic/demersal teleosts (Farré et al., 2016; Friedman et al., 2020), reef fishes (Claverie and Wainwright, 2014), Carangaria (Ribeiro et al., 2018), and characiforms (Burns and Sidlauskas, 2019). Elongation was also identified as a second major axis of morphological variation across 394 morphologically diverse teleost families (Price et al., 2019), and the main axis of body-shape diversification across over 3,000 species of marine teleosts (Martinez et al., 2021).

In some of these studies investigating body-shape diversification in teleosts, body elongation was associated with habitat transitions (e.g., Farré et al., 2016; Martinez et al., 2021) and diet (e.g., Burns and Sidlauskas, 2019). Body elongation is often associated with both diet and habitat (partitioned by depth), with piscivorous stomiiforms (e.g., melanostomiines, chauliodontines, and stomiines) having an elongated body shape with sagittiform morphology and showing the highest morphological disparity in comparison to generalists and zooplanktivorous stomiiforms, in a pattern similar to that found in characiforms (Burns and Sidlauskas, 2019). On the other hand, the generalists and zooplanktivorous stomiiforms greatly vary in body shape, having fusiform body shape (e.g., most maurolicines, the gonostomatids *Cyclothone*, *Margrethia*, and *Zaphotias*, astronesthines, and the phosichthyids *Ichthyococcus* and *Vinciguerria*), elongated body shape (e.g., diplophids, the gonostomatids *Gonostoma* and *Sigmops*, and the phosichthyids *Pollichthys*, *Polymetme*, and *Yarrella*), or deep compressed body shape (e.g., sternoptychines), with the dorsal fin positioned near midbody (e.g., diplophids, gonostomatids, phosichthyids, and most sternoptychids and astronesthines), long anal fin (e.g., gonostomatids, diplophids, most sternoptychids, the phosichthyids *Pollichthys*, *Polymetme*, and *Yarrella*, and the astronesthine *Neonesthes capensis*), and large eye (e.g., sternoptychids, the gonostomatids *Margrethia*, and *Zaphotias*, the phosichthyids *Ichthyococcus* and *Vinciguerria*, the astronesthine *Astronesthes*, and the malacosteine *Malacosteus*).

Table 6. Results from Procrustes ANOVA testing for differences in mean body shape and centroid size (CS) among the Stomiiformes classified by clades, diel vertical migration (DVM), bathymetric distribution (depth), and diet, without and with accounting for phylogeny. Asterisks represent significant differences ($P \leq 0.05$).

	Without phylogeny				With phylogeny			
	F-values		*P*-values		F-values		*P*-values	
Classifiers	Shape	CS	Shape	CS	Shape	CS	Shape	CS
Clades	7.90	4.24	0.002*	0.092	0.99	0.60	0.46	0.58
DVM	0.79	0.16	0.454	0.762	0.51	0.15	0.73	0.65
Depth	1.97	0.29	0.122	0.262	0.27	0.00	0.9	0.97
Diet	14.4	1.01	0.002*	0.23	0.74	0.046	0.65	0.38

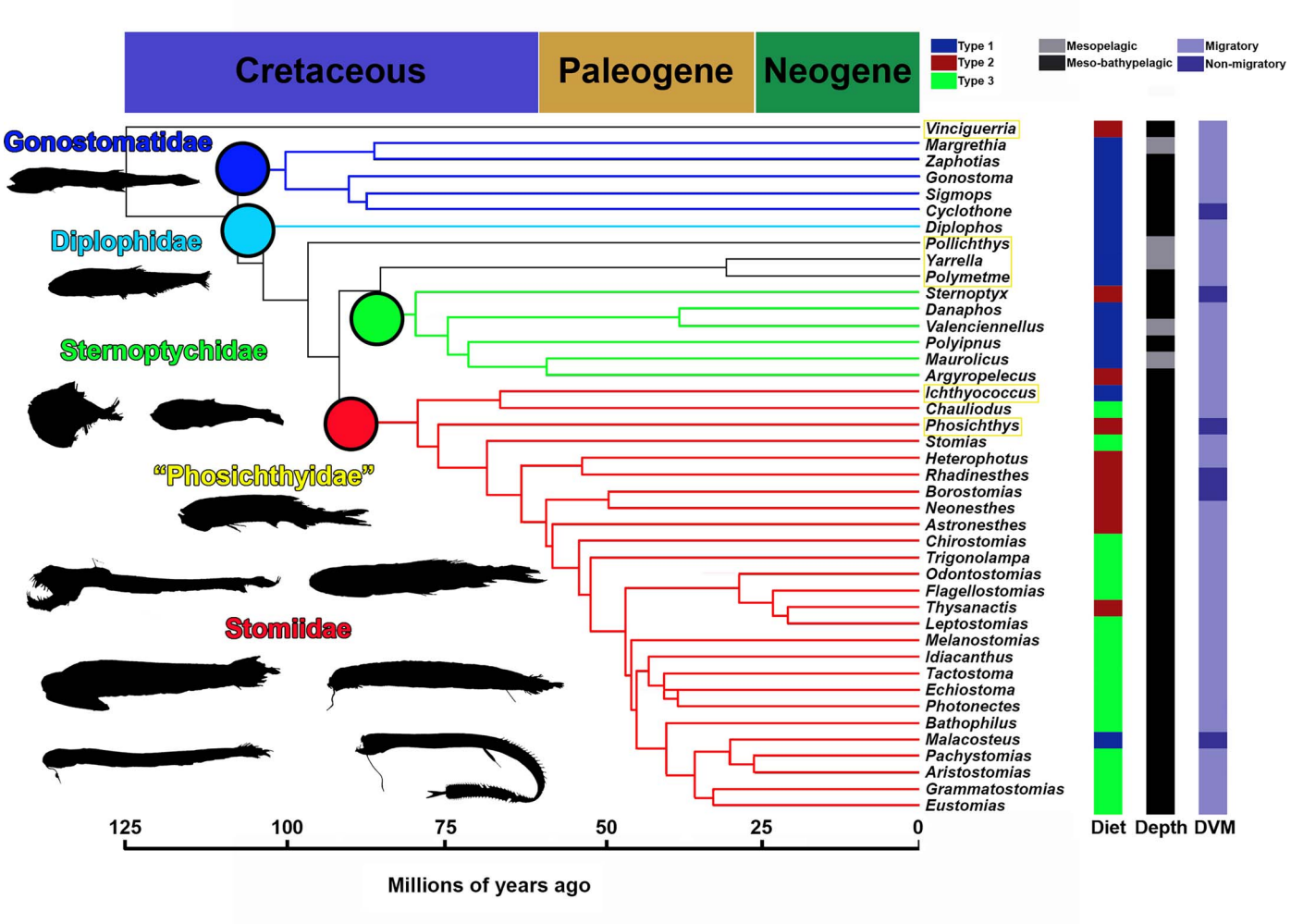

Fig. 7. Time-calibrated phylogenetic tree of the Stomiiformes, adapted from Rabosky et al. (2018), with the ecological traits of diet (type 1 = zooplanktivorous, type 2 = generalists, or type 3 = piscivorous), depth distribution (mesopelagic or meso-bathypelagic), and diel vertical migration pattern (migratory or non-migratory) indicated. The color code on the cladogram indicates families.

Multivariate morphological disparity of meso-bathypelagic stomiiforms exceeds that of strictly mesopelagic stomiiforms (Table 3). The meso-bathypelagic assemblage includes taxa from all major stomiiform clades, while strictly mesopelagic stomiiforms embrace just the maurolicines, which have fusiform bodies, and the sternoptychines, which have deep bodies. While the higher morphological disparity in the meso-bathypelagic species proximally reflects the greater prevalence of elongate forms, their higher diversity may stem simply from the greater phylogenetic breadth and older age of the most recent common ancestor of that assemblage and does not necessarily indicate that elongate bodies evolve more readily in the bathypelagic zone.

That said, Neat and Campbell (2013) reported a trend in the elongation of body shape as depth increases for the deep-sea fishes from the Atlantic Ocean, as did Farré et al. (2016) for the demersal fish assemblages in Mediterranean Sea, Maile et al. (2020) for lizardfishes (Aulopiformes), and Martinez et al. (2021) for several marine teleostean species. Our results and theirs are consistent with the idea that the deep sea is a hot spot of fish body-shape evolution, with elongated deep-sea fishes displaying forms mostly suited to slow swimming (Martinez et al., 2021). Body elongation is usually considered an efficient strategy related to feeding and swimming in deep-sea ecosystems because morphologies suited to low performance swimming may help fishes save scarce energy for reproduction and growth (Neat and Campbell, 2013), and possibly for diel vertical migration. In the case of sagittiform fish, such as pikes and most stomiids, the combined fin area well posterior on the body generates a large amount of burst-speed thrust for prey capture, as demonstrated in a study conducted by Webb (1984). This type of body shape and fin positions well suited to accelerating are advantages in the deep sea, as food resources are limited as depth increases (Pérès, 1985).

Morphological disparity is greater in stomiiforms that do not perform diel vertical migrations than those that do (Table 3). However, among the specimens analyzed, only seven species (ca. 12% of the total) do not migrate on a daily basis, including the gonostomatids *Cyclothone microdon* and *C. pseudopallida*, the phosichthyids *Phosichthys argenteus* and *Yarrella blackfordi*, the sternoptychine *Sternoptyx pseudobscura*, the astronesthines *Borostomias antarcticus* and *Rhadinesthes decimus*, and the malacosteine *Malacosteus australis*. All the non-migrant stomiiforms are generalist or zooplanktivorous feeders, but there is no correlation of position of dorsal and anal fins and body shape (PC1), caudal peduncle and eye size (PC2), or the position of the pelvic fins (PC3) in

the morphospace. Even though we could not find any common trait among the non-migratory species, Schnell et al. (2021) revealed differences in the epaxial and hypaxial musculotendinous system between the migratory and non-migratory species. It is also important to note that the pattern of diel vertical migration among the stomiiforms is more complex than a simple dichotomy of migratory and non-migratory species. For example, some taxa (e.g., *Aristostomias* and *Photostomias*) have asynchronous diel vertical migration, where only a portion of the population migrates upward at night while other individuals remain at greater depths; there are also ontogenetic variations, among other factors (Sutton and Hopkins, 1996; Kenaley, 2008). Additionally, several stomiiforms are rarely collected (e.g., *Opostomias* and *Rhadinesthes*), which makes it difficult to assume a DVM pattern (Kenaley et al., 2014).

Eye size also covaries with body shape, with the fusiform and deep-bodied stomiiforms having large eyes (e.g., the gonostomatid *Margrethia*, the phosichthyids *Ichthyococcus* and *Vinciguerria*, the astronesthine *Astronesthes*, and all sternoptychids) and the elongated stomiiforms having small or moderate eyes (e.g., diplophids, most gonostomatids and phosichthyids, chauliodontines, melanostomiines, and stomiines). Although most elongated stomiiforms with moderate to small eyes are ambush predators (especially the stomiids), we didn't test explicitly whether eye size diminishes during evolutionary transitions to ambush predation, and habitat shifts could provide an alternative explanation. For example, fishes inhabiting depths below 1,000 meters often have relatively small eyes because no downwelling sunlight penetrates to those depths and fishes there tend to rely most heavily on senses other than vision (Munk, 1965; de Busserolles et al., 2014). Most stomiiforms with large eyes are strictly mesopelagic, while the eyes of meso-bathypelagic species vary from small to moderate, with malacosteines providing an exception. In comparison to other mesopelagic fishes, a similar pattern was found in myctophids, in which species inhabiting shallower depths have larger eyes than do those from greater depths (de Busserolles et al., 2014). Those large eyes increase the chance of capturing bioluminescent flashes and faint sunlight, thereby allowing detection of body silhouettes. However, the small eyes of many bathypelagic fishes can still provide ample vision (Warrant, 2000; Warrant et al., 2003; de Busserolles et al., 2014). Many small-eyed species have frontally directed foveae of high anatomical acuity (e.g., alepocephalids; Wagner et al., 1998) and large pupils, providing sufficient sensitivity and resolution to locate bioluminescent flashes up to several tens of meters away (Wagner et al., 1998; Warrant, 2000; Warrant et al., 2003). Thus, although the pattern of large eye associated with inhabiting shallower depths has been observed in the Stomiiformes and Myctophiformes, more studies are necessary to understand whether eye size relates most strongly with prey capture, depth, vertical migration, or even with predation avoidance.

Although the Stomiidae is the most species-rich family in the Stomiiformes, the Sternoptychidae is the most morphologically diverse, and both families have similar crown clade ages of about 75 million years, implying that their difference in disparity does not simply result from unequal ages. The Sternoptychidae includes forms varying from fusiform as in *Argyripnus*, *Danaphos*, *Maurolicus*, and *Valenciennellus*, to elongated species like *Araiophos* and *Thorophos*—the former includes the slenderest species within the family. However, the most remarkable forms are the hatchetfishes *Argyropelecus*, *Polyipnus*, and *Sternoptyx*, which have a deep, laterally compressed body shape. That form is unusual for pelagic fishes and more frequent in demersal fishes (e.g., Friedman et al., 2020; Larouche et al., 2020), and is thought to enhance maneuverability (Webb, 1984), although this might not be the case in sternoptychids. In terms of ecological aspects, sternoptychids include only zooplanktivorous and generalist species (Hopkins et al., 1996; Carmo et al., 2015; Eduardo et al., 2020), but not strictly piscivorous species, and are either mesopelagic or meso-bathypelagic, with most species performing diel vertical migration, except *Sternoptyx* (Badcock, 1970; Gon, 1990; Mundy, 2005; Fahay, 2007; Eduardo et al., 2020).

Phylogenetic patterns.—Analyzing the time-calibrated phylogeny (Rabosky et al., 2018; Fig. 7), it is possible to infer that the hypothetical common ancestor of the Stomiiformes has an elongated body, with a long anal fin. It is also possible to observe a transition from a dorsal fin positioned at midbody in gonostomatids and sternoptychids to a posteriorly placed dorsal fin in most sagittiform stomiids.

The Stomiiformes first appeared at the end of the Early Cretaceous at 117.3 Ma, and the diversification of crown stomiiforms began during the Late Cretaceous (~91 million years ago), with the oldest known fossil taxon, *Paravinciguerria praecursor*, from the Cenomanian–Turonian boundary, assumed to be a stem stomiiform (Carnevale and Rindone, 2011; Kenaley et al., 2014). It is interesting to notice the existence of two divergent hypothesis of the stomiid origin, with Kenaley et al. (2014) suggesting that the dragonfishes appeared during the Late Eocene (ca. ~35 Ma) and Rabosky et al. (2018) during the Late Cretaceous (ca. ~75 Ma).

The lightfishes belonging to the polyphyletic family Phosichthyidae are an interesting case of phylomorphospace occupation. Even though the Phosichthyidae was not recovered as monophyletic in recent molecular phylogenies (Kenaley et al., 2014; Betancur-R. et al., 2017; Mirande, 2017; Rabosky et al., 2018), this name is still in use (e.g., Nelson, 2006; Nelson et al., 2016; Sutton et al., 2020; Villarins et al., 2022). According to Rabosky et al. (2018), *Vinciguerria* is sister to all stomiiforms, *Pollichthys* is sister to a clade formed by *Polymetme*, *Yarrella*, and the Sternoptychidae, and another clade formed by *Ichthyococcus*, *Phosichthys*, and members of the Stomiidae. In the phylomorphospace, phosichthyids occupy two distinct regions. One region includes *Pollichthys*, *Polymetme*, and *Yarrella*. These species have slender bodies, small to moderate eyes, and long anal fins, and they feed mainly on small crustaceans, especially the euphausiids. The second region includes *Ichthyococcus*, *Phosichthys*, and *Vinciguerria*. These have deep bodies, large eyes, and a short anal fin, and are generalist feeders.

The astronesthines *Astronesthes*, *Neonesthes*, and *Rhadinesthes*, and the phosichthyids *Ichthyococcus*, *Phosichthys*, and *Vinciguerria* clustered around the consensus configuration in the phylomorphospace and were comparatively more restricted in body shape than other taxa, such as the sagittiform stomiids and the deep-bodied sternoptychines, which have significantly higher variance and disparity in body shape. The fusiform body shape and a mid-body position of the dorsal fin are the main traits distinguishing the astronesthines from other stomiids (Weitzman, 1967; Fink, 1985). A closer relationship between the Astronesthinae and Phosichthyidae was suggested by Weitzman (1967) based on morphological similarities

related to the skull, including the upper jaw, teeth, and the ethmoid region. However, such relationships were never recovered using molecular evidence, which has consistently rendered the Astronesthinae as a clade within the Stomiidae (Betancur-R. et al., 2017; Mirande, 2017; Rabosky et al., 2018). However, unlike most stomiids, the astronesthines are generalists, feeding mainly on small crustaceans such as krill and decapods, and minorly on fish (Clarke, 1982; Gibbs, 1984; Hopkins et al., 1996; Sutton and Hopkins, 1996). This feeding habit is similar to the species currently allocated in the Phosichthyidae (Hopkins et al., 1996; Sutton and Hopkins, 1996).

The substantial phylogenetic signal in body shape and size within stomiiforms means that closely related taxa tended to cluster in the phylomorphospace due to their shared evolutionary history (Fig. 6). The high phylogenetic signal in body shape ($K = 1.9$) substantially exceeded the expectation of $K = 1$ under neutral evolution or genetic drift (Kamilar and Cooper, 2013). Such high values are often interpreted as evolutionary or phylogenetic conservatism (Losos, 2008) and reflect the tendency of species to retain their ancestral traits. The existence of several distinct clusters suggests the existence of multiple adaptive peaks within the stomiiform morphospace. While this could explain why lineages tend not to leave particular regions once they have occupied them, testing that conjecture would require model testing in a more densely sampled phylomorphospace and hence a phylogeny with greater taxon sampling.

Inclusion of the phylogeny eroded the significance of differences in morphological disparity and mean shape among stomiiform ecological classes that the non-phylogenetic analysis returned. The fact that the significant correlations between body shape and ecological traits disappear after accounting for phylogeny could indicate that these ecological traits have not substantially shaped morphological evolution in the Stomiiformes. However, it may also be that ecological traits played a role only during the early evolution of the group or that the current dataset lacks the statistical power to uncover any relationship that may exist between shifts in depth, diet, or migration and the shape diversification of stomiiforms. The lack of significance could also stem from the relatively few transitions among ecological classes that occurred during stomiiform evolution, or from the relatively sparse taxon sampling of the phylogenetically informed analysis. As such, results herein should not be taken as proof of a lack of ecological influence on morphological diversification, but rather as a call for further investigation.

Conclusion.—The complex evolutionary history of the Stomiiformes after they colonized the deep sea involves marked diversification of body shape, resulting in a radiation that spans mesopelagic generalists with fusiform bodies and the sagittiform or anguilliform meso-bathypelagic piscivores that are the most iconic living dragonfishes. The most important axis of variation within the Stomiiformes involves the size and position of the dorsal and anal fins, followed by axes describing body size and body depth. There is an overall trend toward meso-bathypelagic taxa having more elongate bodies than strictly mesopelagic ones, though the compressiform mesopelagic hatchetfishes in the Sternoptychidae represent a notable exception. While some extremely elongate stomiiforms also possess long anal and dorsal fins, elongation of the body does not mandate fin elongation. Some elongate species have short dorsal fins and long anal fins (e.g., *Eustomias*), while elongate sagittiform taxa like *Aristostomias* have short, posteriorly placed dorsal and anal fins. Those sagittiform taxa are typically piscivores with large mouths and small to moderately sized eyes. In contrast, generalist and zooplanktivorous stomiiforms vary more in body shape, encompassing fusiform, elongate, and deep-bodied morphologies. There is significant association between shape and ecological traits (e.g., generalists and piscivorous stomiiforms have a higher morphological disparity than the zooplanktivorous counterparts). However, the degree of shared ancestry strongly predicts similarity of body shape within the Stomiiformes, and thus the inclusion of phylogeny eroded the significance of differences in morphological disparity among ecological groups. The disappearance of significant correlations between shape and ecological traits after accounting for phylogeny might indicate that ecological traits played little role in shaping morphological evolution. However, the lack of significance could stem from the relatively sparse taxon sampling of the phylogenetically informed analysis or suggest that shifts between niches were too infrequent for the analysis to uncover statistically a significant link between ecology and morphology that may nevertheless exist. Future research should revisit this question once a more detailed phylogeny of the Stomiiformes becomes available.

MATERIAL EXAMINED

Araiophos eastropas: SIO 90-177 (4).

Argyripnus atlanticus: MNRJ 30552 (10).

Argyropelecus aculeatus: MZUSP 78245 (1), MZUSP 80271 (2), MZUSP 86374 (1), MZUSP 86376 (4), MZUSP 86698 (3), MZUSP 129727 (1), MZUSP 129886 (1), MZUSP 129887 (1).

Argyropelecus affinis: OSIC 6424 (1), OSIC 14136 (2), OSIC 14155 (1), OSIC 19956 (1), OSIC 19957 (2), OSIC 22684 (1).

Aristostomias scintillans: OSIC 14209 (1), OSIC 14458 (1), OSIC 14475 (1), OSIC 14477 (1), OSIC 14557 (1), OSIC 14576 (1), OSIC 14701 (1).

Astronesthes gemmifer: USNM 45448 (1), USNM 436537 (1).

Astronesthes macropogon: MNRJ 30792 (1), MNRJ 30793 (2), MNRJ 30794 (5), MNRJ 30797 (2), MNRJ 30800 (2), MZUSP 78244 (2), MZUSP 80272 (1), MZUSP 80531 (1), MZUSP 80532 (1).

Bathophilus flemingi: OSIC 14294 (1), OSIC 14479 (1), OSIC 14556 (1), OSIC 14559 (1), OSIC 14567 (1), OSIC 14568 (1), OSIC 14569 (1), OSIC 14580 (1), OSIC 14585 (1), OSIC 14605 (1), OSIC 14616 (1), OSIC 14619 (1).

Borostomias antarcticus: SIO 61-45 (1), USNM 265384 (2), USNM 300019 (1), USNM 454835 (3).

Chauliodus danae: MZUSP 128733 (2).

Chauliodus macouni: OSIC 921 (1), OSIC 8673 (1), OSIC 11347 (1), OSIC 11763 (1), OSIC 11823 (2), OSIC 13686 (1), OSIC 14153 (2), OSIC 14834 (3), OSIC 17304 (1).

Chauliodus sloani: MNRJ 42816 (1), MNRJ 42817 (2), MNRJ 42820 (1).

Chirostomias pliopterus: MCZ 132707 (1), MCZ 132709 (1).

Cyclothone microdon: OSIC 11279 (4), OSIC 11346 (4), OSIC 14427 (1).

Cyclothone pseudopallida: MZUSP 129716 (14).

Danaphos oculatus: OSIC 11861 (1), OSIC 11867 (1), OSIC 11913 (1).

Diplophos taenia: MZUSP 78235 (1), MZUSP 80530 (1), OSIC 11853 (2), SIO 11-203 (1), SIO 69-334 (1), SIO 77-218 (2).

Echiostoma barbatum: USNM 235659 (2), USNM 358644 (1), USNM 409549 (1), USNM 436522 (1).

Eustomias filifer: MCZ 96167 (1), MCZ 153128 (2).

Flagellostomias boureei: SIO 74-20 (1), SIO 76-107 (1), USNM 234681 (1), USNM 234682 (1), USNM 297019 (1), USNM 322976 (1).

Gonostoma atlanticum: OSIC 11844 (2).

Grammatostomias flagellibarba: MCZ 153118 (1), MCZ 164122 (1).

Heterophotus ophistoma: MNRJ 30914 (1), SIO 20-38 (1), SIO 70-341 (1), SIO 73-165 (1), USNM 214461 (1), USNM 258818 (3).

Ichthyococcus elongatus: OSIC 11820 (1), OSIC 11848 (1), OSIC 11872 (1), OSIC 14295 (1).

Idiacanthus atlanticus: MZUSP 78406 (6), MZUSP 86603 (2).

Leptostomias gladiator: MCZ 149495 (1), MCZ 155381 (1), MCZ 169550 (1), MNRJ 30806 (1), OSIC 14551 (1), OSIC 14575 (1).

Malacosteus australis: MNRJ 30386 (1), MNRJ 30723 (1), MNRJ 30728 (1), MNRJ 30733 (1), MNRJ 30737 (1), MNRJ 30740 (2), MZUSP 129890 (1), MZUSP 129891 (2).

Manducus maderensis: MCZ 61476 (1), MCZ 91350 (1), MNRJ 30128 (8), MNRJ 30136 (6), MNRJ 30135 (2), MNRJ 30154 (1), MNRJ 30157 (1), MNRJ 30301 (1).

Margrethia obtusirostra: USNM 248767 (2), USNM 248768 (1), USNM 248771 (2).

Maurolicus stehmanni: MZUSP 80238 (10).

Maurolicus weitzmani: USNM 391391 (1), USNM 391455 (1).

Melanostomias melanops: MCZ 148622 (1), MCZ 164745 (1), MNRJ 30893 (2), MNRJ 30895 (2), MNRJ 30904 (1), MNRJ 44092 (1), MNRJ 50693 (1).

Neonesthes capensis: USNM 454448 (2).

Odontostomias micropogon: MCZ 58810 (1), MCZ 132152 (1), USNM 326567 (1), USNM 326568 (1).

Opostomias mitsuii: OSIC 14482 (1), OSIC 14550 (3), OSIC 14565 (1), OSIC 14571 (1), OSIC 14623 (1), OSIC 14651 (1), OSIC 14668 (1), OSIC 14673 (1), OSIC 14686 (1).

Pachystomias microdon: USNM 296691 (2), USNM 297922 (3).

Phosichthys argenteus: MCZ 61171 (1), MCZ 140441 (1), MZUSP 78249 (6), MZUSP 86420 (1), MZUSP 86652 (2), MZUSP 86653 (2), MZUSP 86731 (2).

Photonectes margarita: OSIC 014658 (1), SIO 11-410 (1), SIO 97-104 (1), SIO 98-5 (1), USNM 201740 (1), USNM 234360 (1), USNM 234374 (1).

Photostomias guernei: MCZ 131727 (5), MNRJ 30743 (1).

Pollichthys mauli: MZUSP 78229 (3), MZUSP 80335 (1), MZUSP 80337 (1), MZUSP 80345 (6), MZUSP 86691 (4).

Polyipnus laternatus: MCZ 40574 (1), MCZ 91010 (1).

Polyipnus spinifer: USNM 135514 (3).

Polymetme thaeocoryla: MZUSP 86401 (10), MZUSP 86412 (5), MZUSP 86650 (6), USNM 304218 (3), USMN 407426 (1).

Rhadinesthes decimus: MCZ 64832 (1), OSIC 11650 (1), OSIC 11651 (1).

Sigmops elongatus: MNRJ 30270 (1), MNRJ 30271 (1), MNRJ 30276 (1), MNRJ 42846 (3), MNRJ 46049 (1), MNRJ 46061 (1), MNRJ 46063 (1), MNRJ 46065 (1), MZUSP 78221 (1), MZUSP 80527 (1), MZUSP 80528 (1), MZUSP 86606 (2), MZUSP 129718 (8), MZUSP 129885 (1).

Sternoptyx pseudobscura: MNRJ 30159 (1), MNRJ 30167 (8), MNRJ 30162 (1), MNRJ 3016 (1), MNRJ 50153 (1), MZUSP 129888 (1), MZUSP 129889 (1), OSIC 12858 (8).

Stomias affinis: MZUSP 48982 (1), MZUSP 86572 (3), MZUSP 86574 (2), MZUSP 86575 (2), MZUSP 86719 (1), MZUSP 129876 (1), MZUSP 129877 (1), MZUSP 129880 (1), MZUSP 129898 (5).

Tactostoma macropus: OSIC 9181 (1), OSIC 11301 (8), OSIC 11342 (4), OSIC 14558 (1), OSIC 14654 (6), OSIC 14653 (1), OSIC 14654 (1), OSIC 14927 (1).

Thorophos nexilis: USNM 92326 (1).

Thysanactis dentex: USNM 365806 (4), USNM 365808 (1).

Trigonolampa miriceps: MCZ 124655 (1), MCZ 137986 (1), MCZ 165921 (1).

Valenciennellus tripunctulatus: MZUSP 129731 (1), OSIC 14881 (1).

Vinciguerria nimbaria: MZUSP 78227 (3), MZUSP 80287 (4), MZUSP 80330 (6), MZUSP 129723 (1), OSIC 11874 (3), OSIC 11877 (5), OSIC 11882 (1).

Vinciguerria poweriae: MZUSP 80533 (8).

Yarrella blackfordi: MCZ 124870 (1), MCZ 126580 (2).

Zaphotias pedaliotus: MCZ 58629 (5), SIO 63-560 (3).

DATA ACCESSIBILITY

Supplemental material is available at https://www.ichthyologyandherpetology.org/i2023068. Unless an alternative copyright or statement noting that a figure is reprinted from a previous source is noted in a figure caption, the published images and illustrations in this article are licensed by the American Society of Ichthyologists and Herpetologists for use if the use includes a citation to the original source (American Society of Ichthyologists and Herpetologists, the DOI of the *Ichthyology & Herpetology* article, and any individual image credits listed in the figure caption) in accordance with the Creative Commons Attribution CC BY License.

ACKNOWLEDGMENTS

We thank the following people and institutions for providing specimens: Aléssio Datovo, Mario C. C. de Pinna, Osvaldo Oyakawa, and Michel D. Gianeti from Museu de Zoologia, Universidade de São Paulo (MZUSP), Cristiano L. R. Moreira, Marcelo R. Britto, and Paulo A. Buckup from Museu Nacional, Universidade Federal do Rio de Janeiro (MNRJ), Peter Konstantinidis from the Oregon State Ichthyology Collection, Oregon State University (OS), Meaghan Sorce and George Lauder from the Museum of Comparative Zoology, Harvard University (MCZ), Benjamin Frable from Scripps Institution of Oceanography, University of California San Diego (SIO), Lynne Parenti and Diane Pitassy from National Museum of Natural History, Smithsonian Institution (USNM), the crew of the R/V *Alpha Crucis* under the command of José Rezende during the cruises of the DEEP OCEAN Project, and Marcos O. C. Santos for the specimens collected by the RV *Alucia*. Funding support was provided by CNPq (AAG, Ph.D. scholarship process 159146/2018-6), and CAPES (PrInt scholarship, AAG, process 88887.571899/2020-00), and FAPESP (MRSM, DEEP OCEAN project, process 2017/12909-4; RAC, fellowship, process 2022/14954-5). We gratefully acknowledge the members of the Sidlauskas Lab, Oregon State University (OSU), and the DEEP Lab, Instituto Oceanográfico, Universidade de São Paulo (IOUSP) for all support given during the development of this work, and Bruno G. Augusta (MZUSP) for image editing and comments on this manuscript.

LITERATURE CITED

Angel, M. V. 1997. What is the deep-sea?, p. 2–41. *In*: Deep-Sea Fishes D. J. Randall and A. P. Farrell (eds.). Academic Press, San Diego.

Badcock, J. 1970. The vertical distribution of mesopelagic fishes collected on the SOND cruise. Journal of the Marine Biological Association of the United Kingdom 50:1001–1044.

Baken, E. K., M. L. Collyer, A. Kaliontzopoulou, and D. C. Adams. 2021. geomorph v4. 0 and gmShiny: enhanced analytics and a new graphical interface for a comprehensive morphometric experience. Methods in Ecology and Evolution 12:2355–2363.

Betancur-R, R., E. O. Wiley, G. Arratia, A. Acero, N. Bailly, M. Miya, G. Lecointre, and G. Ortí. 2017. Phylogenetic classification of bony fishes. BMC Evolutionary Biology 17:162.

Blomberg, S. P., T. Garland, and A. R. Ives. 2003. Testing for phylogenetic signal in comparative data: behavioral traits are more labile. Evolution 57:717–745.

Bookstein, F. L. 1991. Morphometric Tools for Landmark Data: Geometry and Biology. Cambridge University Press, Cambridge.

Burns, M. D., and B. L. Sidlauskas. 2019. Ancient and contingent body shape diversification in a hyperdiverse continental fish radiation. Evolution 73:569–587.

de Busserolles, F., N. J. Marshall, and S. P. Collin. 2014. The eyes of lanternfishes (Myctophidae, Teleostei): novel ocular specializations for vision in dim light. Journal of Comparative Neurology 522:1618–1640.

Carmo, V., T. Sutton, G. Menezes, T. Falkenhaug, and O. A. Bergstad. 2015. Feeding ecology of the Stomiiformes (Pisces) of the northern Mid-Atlantic Ridge. 1. The Sternoptychidae and Phosichthyidae. Progress in Oceanography 130:172–187.

Carnevale, G., and A. Rindone. 2011. The teleost fish *Paravinciguerria praecursor* Arambourg, 1954 in the Cenomanian of north-eastern Sicily. Bollettino della Società Paleontologica Italiana 50:1–10.

Clarke, T. A. 1982. Feeding habits of stomiatoid fishes from Hawaiian waters. Fishery Bulletin 80:287–304.

Claverie, T., and P. C. Wainwright. 2014. A morphospace for reef fishes: elongation is the dominant axis of body shape evolution. PLoS ONE 9:e112732.

Denton, J. S. S., and D. C. Adams. 2015. A new phylogenetic test for comparing multiple high-dimensional evolutionary rates suggests interplay of evolutionary rates and modularity in lanternfishes (Myctophiformes; Myctophidae). Evolution 69:2425–2440.

Eduardo, L. N., A. Bertrand, M. M. Mincarone, L. V. Santos, T. Fredou, R. V. Assunção, A. Silva, F. Ménard, R. Schwamborn, F. Le Loc'h, and F. Lucena-Frédou. 2020. Hatchetfishes (Stomiiformes: Sternoptychidae) biodiversity, trophic ecology, vertical niche partitioning and functional roles in the western Tropical Atlantic. Progress in Oceanography 187:102389.

Fahay, M. P. 2007. Early Stages of Fishes in the Western North Atlantic Ocean (Davis Strait, Southern Greenland and Flemish Cap to Cape Hatteras). Volume 1: Acipenseriformes through Syngnathiformes. Northwest Atlantic Fisheries Organization, Halifax, Nova Scotia.

Farré, M., A. Lombarte, L. Recasens, F. Maynou, and V. M. Tuset. 2015. Habitat influence in the morphological diversity of coastal fish assemblages. Journal of Sea Research 99:107–117.

Farré, M., V. M. Tuset, J. E. Cartes, E. Massutí, and A. Lombarte. 2016. Depth-related trends in morphological and functional diversity of demersal fish assemblages in the western Mediterranean Sea. Progress in Oceanography 147:22–37.

Fink, W. L. 1985. Phylogenetic interrelationships of the stomiid fishes (Teleostei: Stomiiformes). Miscellaneous Publications, Museum of Zoology, The University of Michigan 171:1–127.

Fricke, R., W. N. Eschmeyer, and R. Van Der Laan (Eds.). 2023. Eschmeyer's Catalog of Fishes: Genera, Species, References. http://researcharchive.calacademy.org/research/

ichthyology/catalog/fishcatmain.asp. Electronic version accessed 22 April 2020.

Friedman, S. T., S. A. Price, K. A. Corn, O. Larouche, C. M. Martinez, and P. C. Wainwright. 2020. Body shape diversification along the benthic–pelagic axis in marine fishes. Proceedings of the Royal Society B 287:20201053.

Gannon, D. R., J. E. Craddock, and A. J. Read. 1998. Autumn food habits of harbor porpoises, *Phocoena phocoena*, in the Gulf of Maine. Fishery Bulletin 96:428–437.

Gartner J. V., Jr., R. E. Crabtree, and K. J. Sulak. 1997. Feeding at depth, p. 115–193. *In*: Fish Physiology. Volume 16. D. J. Randall and A. P. Farrell (eds.). Academic Press, Cambridge, Massachusetts.

Gibbs R. H., Jr. 1984. Stomiidae, p. 338–340. *In*: Fishes of the North-eastern Atlantic and the Mediterranean. Vol. 1. P. J. P. Whitehead, M. L. Bauchot, J. C. Hureau, J. Nielsen, and E. Tortonese (eds.). UNESCO, Paris.

Gon, O. 1990. Stomiidae. Scaly dragonfishes, p. 127–133. *In*: Fishes of the Southern Ocean. O. Gon and P. C. Heemstra (eds.). J.L.B. Smith Institute of Ichthyology, Grahamstown, South Africa.

Goswami, A., A. Watanabe, R. N. Felice, C. Bardua, A. C. Fabre, and P. D. Polly. 2019. High-density morphometric analysis of shape and integration: the good, the bad, and the not-really-a-problem. Integrative and Comparative Biology 59:669–683.

Harold, A. S. 2002. Gonostomatidae, p. 881–884, Phosichthyidae, p. 885–888, Sternoptychidae, p. 889–892, Astronesthidae, p. 893–895, Chauliodontidae, p. 896–898, Idiacanthidae, p. 899–900, Malacosteidae, p. 901–903, Stomiidae, p. 904–906, and Melanostomiidae, p. 907–912. *In*: The Living Marine Resources of the Western Central Atlantic, FAO Species Identification Guide for Fishery Purposes. Vol. 2. K. E. Carpenter (ed.). FAO, Rome.

Harold, A. S., and S. H. Weitzman. 1996. Interrelationships of stomiiform fishes, p. 333–353. *In*: Interrelationships of Fishes M. L, J Stiassny, L. R. Parenti, and G. D. Johnson (eds.). Academic Press Inc., San Diego, California.

Herring, P. J. 2007. Sex with the lights on? A review of bioluminescent sexual dimorphism in the sea. Journal of the Marine Biological Association of the United Kingdom 87:829–842.

Hopkins, T. L., T. T. Sutton, and T. M. Lancraft. 1996. The trophic structure and predation impact of a low latitude midwater fish assemblage. Progress in Oceanography 38:205–239.

Kamilar, J. M., and N. Cooper. 2013. Phylogenetic signal in primate behavior, ecology and life history. Philosophical Transactions of the Royal Society B 368:20120341.

Kenaley, C. P. 2008. Diel vertical migration of the loosejaw dragonfishes (Stomiiformes: Stomiidae: Malacosteinae): a new analysis for rare pelagic taxa. Journal of Fish Biology 73:888–901.

Kenaley, C. P. 2009. Revision of Indo-Pacific species of the loosejaw dragonfish genus *Photostomias* (Teleostei: Stomiidae: Malacosteinae). Copeia 2009:175–189.

Kenaley, C. P., S. C. Devaney, and T. T. Fjeran. 2014. The complex evolutionary history of seeing red: molecular phylogeny and the evolution of an adaptive visual system in deep-sea dragonfishes (Stomiiformes: Stomiidae). Evolution 68:996–1013.

Larouche, O., B. Benton, K. A. Corn, S. T. Friedman, D. Gross, M. Iwan, B. Kessler, C. M. Martinez, S. Rodriguez, H. Whelpley, P. C. Wainwright, and S. A. Price. 2020. Reef-associated fishes have more maneuverable body shapes at a macroevolutionary scale. Coral Reefs 39:1427–1439.

Losos, J. B. 2008. Phylogenetic niche conservatism, phylogenetic signal and the relationship between phylogenetic relatedness and ecological similarity among species. Ecology Letters 11:995–1007.

Maile, A. J., Z. A. May, E. S. DeArmon, R. P. Martin, and M. P. Davis. 2020. Marine habitat transitions and body-shape evolution in lizardfishes and their allies (Aulopiformes). Copeia 108:820–832.

Marranzino, A. N., and J. F. Webb. 2018. Flow sensing in the deep sea: the lateral line system of stomiiform fishes. Zoological Journal of the Linnean Society 183:945–965.

Martinez, C. M., S. T. Friedman, K. A. Corn, O. Larouche, S. A. Price, and P. C. Wainwright. 2021. The deep sea is a hot spot of fish body shape evolution. Ecology Letters 24:1788–1799.

Mindel, B. L., F. C. Neat, C. N. Trueman, T. J. Webb, and J. L. Blanchard. 2016. Functional, size and taxonomic diversity of fish along a depth gradient in the deep sea. PeerJ 4:e2387.

Mirande, J. M. 2017. Combined phylogeny of ray-finned fishes (Actinopterygii) and the use of morphological characters in large-scale analyses. Cladistics 33:333–350.

Mundy, B. C. 2005. Checklist of the fishes of the Hawaiian Archipelago. Bishop Museum Bulletin in Zoology 6:1–704.

Munk, O. 1965. Ocular degeneration in deep-sea fishes. Galathea Report 8:21–31.

Neat, F. C., and N. Campbell. 2013. Proliferation of elongate fishes in the deep sea. Journal of Fish Biology 83:1576–1591.

Nelson, J. S. 2006. Fishes of the World. Fourth edition. John Wiley and Sons, Inc., Hoboken, New Jersey.

Nelson, J. S., T. C. Grande, and M. V. H. Wilson. 2016. Fishes of the World. Fifth edition. John Wiley and Sons, Inc., Hoboken, New Jersey.

Nunes, J. L. S., N. M. Piorski, and M. E. Araújo. 2008. Phylogenetic and ecological inference of three *Halichoeres* (Perciformes: Labridae) species through geometric morphometrics. Cybium 32:165–171.

Orlov, A., and C. Binohlan. 2009. Length–weight relationships of deep-sea fishes from the western Bering Sea. Journal of Applied Ichthyology 25:223–227.

Paradis, E., J. Claude, and K. Strimmer. 2004. APE: analyses of phylogenetics and evolution in R language. Bioinformatics 20:289–290.

Parin, N. V., and O. D. Borodulina. 2003. Phylogeny, systematics, and zoogeography of the mesopelagic genus *Astronesthes* (Astronesthidae, Stomiiformes). Voprosy Ikhtiologii 43:581–601. [In Russian. English translation in Journal of Ichthyology 43:557–576]

Pérès, J. M. 1985. History of the Mediterranean biota and the colonization of the depths, p. 198–232. *In:* Key Environments: Western Mediterranean. R. Margalef (ed.). Pergamon Press, New York.

Pietsch, T. W. 2009. Oceanic Anglerfishes: Extraordinary Diversity in the Deep Sea. University of California Press, Berkeley and Los Angeles, California.

Price, S. A., S. T. Friedman, K. A. Corn, C. M. Martinez, O. Larouche, and P. C. Wainwright. 2019. Building a body

shape morphospace of teleostean fishes. Integrative and Comparative Biology 59:716–730.

Pulcini, D., C. Costa, J. Aguzzi, and S. Cataudella. 2008. Light and shape: a contribution to demonstrate morphological differences in diurnal and nocturnal teleosts. Journal of Morphology 269:375–385.

R Core Team. 2023. R: a language and environment for statistical computing. R Foundation for Statistical Computing, Vienna, Austria. https://www.R-project.org/

Rabosky, D. L., J. Chang, P. O. Title, P. F. Cowman, L. Sallan, M. Friedman, K. Kaschner, C. Garilao, T. J. Near, M. Coll, and M. E. Alfaro. 2018. An inverse latitudinal gradient in speciation for marine fishes. Nature 559:392–395.

Revell, L. J. 2012. Phytools: an R package for phylogenetic comparative biology (and other things). Methods in Ecology and Evolution 3:217–223.

Ribeiro, E., A. M. Davis, R. A. Rivero-Vega, G. Ortí, and R. Betancur-R. 2018. Post-Cretaceous bursts of evolution along the benthic–pelagic axis in marine fishes. Proceedings of the Royal Society B 285:20182010.

Rohlf, F. J. 2015. The tps series of software. Histrix 26:9–12.

Rohlf, F. J. 2018. tpsDig2. Department of Ecology and Evolution, State University of New York at Stony Brook. Version 2.49. Available at: https://www.sbmorphometrics.org/soft-dataacq.html

Schnell, N. K., J. Kriwet, F. A. López-Romero, G. Lecointre, and C. Pfaff. 2021. Musculotendinous system of mesopelagic fishes: Stomiiformes (Teleostei). Journal of Anatomy 240:1095–1126.

Sidlauskas, B. 2008. Continuous and arrested morphological diversification in sister clades of characiform fishes: a phylomorphospace approach. Evolution 62:3135–3156.

Sutton, T. T. 2013. Vertical ecology of the pelagic ocean: classical patterns and new perspectives: vertical ecology of the pelagic ocean. Journal of Fish Biology 83:1508–1527.

Sutton, T. T., and T. L. Hopkins. 1996. Trophic ecology of the stomiid (Pisces: Stomiidae) fish assemblage of the eastern Gulf of Mexico: strategies, selectivity and impact of a top mesopelagic predator group. Marine Biology 127:179–192.

Sutton, T. T., P. A. Hulley, R. Wienerroither, D. Zaera-Perez, and J. R. Paxton. 2020. Identification Guide to the Mesopelagic Fishes of the Central and Southeast Atlantic Ocean. FAO Species Identification Guide for Fishery Purposes, FAO, Rome.

Tchernavin, V. V. 1953. The Feeding Mechanisms of a Deep-Sea Fish: *Chauliodus sloani* Schneider. British Museum (Natural History), London.

Thistle, D. 2003. The deep-sea floor, an overview, p. 5–37. *In*: Ecosystems of the World 28. Ecosystems of the Deep Oceans. P. A. Tyler (ed.). Elsevier, Amsterdam.

Tuset, V. M., M. Pilar-Olivar, J. L. Otero-Ferrer, C. López-Pérez, P. A. Hulley, and A. Lombarte. 2018. Morpho-functional diversity in *Diaphus* spp. (Pisces: Myctophidae) from the central Atlantic Ocean: ecological and evolutionary implications. Deep-Sea Research Part I: Oceanographic Research Papers 138:46–59.

Villarins, B. T., F. Di Dario, L. N. Eduardo, F. Lucena-Frédou, A. Bertrand, A. M. Prokofiev, and M. M. Mincarone. 2022. Deep-sea dragonfishes (Teleostei: Stomiiformes) collected from off northeastern Brazil, with a review of the species reported from the Brazilian Exclusive Economic Zone. Neotropical Ichthyology 20:e220004.

Wagner, H.-J., E. Fröhlich, K. Negishi, and S. P. Collin. 1998. The eyes of deep-sea fish. II. Functional morphology of the retina. Progress in Retinal and Eye Research 17:637–685.

Warrant, E. 2000. The eyes of deep-sea fishes and the changing nature of visual scenes with depth. Philosophical Transactions of the Royal Society B 355:1155–1159.

Warrant, E. J., S. P. Collin, and N. A. Locket. 2003. Eye design and vision in deep-sea fishes, p. 303–322. *In*: Sensory Processing in Aquatic Environments. S. P. Collin and N. J. Marshall (eds.). Springer, New York.

Webb, P. W. 1984. Form and function in fish swimming. Scientific American 251:72–83.

Weitzman, J. J. 1967. The osteology and relationships of the Astronesthidae, a family of oceanic Fishes. Dana Report 71:1–54.

Wickham, H. 2016. ggplot2: Elegant Graphics for Data Analysis. Springer-Verlag, New York.

Young, J. W., T. D. Lamb, D. Le, R. W. Bradford, and A. W. Whitelaw. 1997. Feeding ecology and interannual variations in diet of southern bluefin tuna, *Thunnus maccoyii*, in relation to coastal and oceanic waters off eastern Tasmania, Australia. Environmental Biology of Fishes 50:275–291.